

# Digital Topology : A survey of 3D object representation and its configuration space.

I. VAKALIS

EC-JRC 21020 Ispra (VA)

Institute for Systems, Informatics and Safety

ITALY

ioannis.vakalis@jrc.it

*Abstract:* The collision avoidance and path planning problem is examined in terms of digital topology. We assume that an object is represented by a 3D digital “image”. The unit cell in this case is a cube and an object can occupy a number of cells in  $\mathbb{R}^3$  space. We also assume that its configuration space is digitized by cubes. Thus space  $\mathbb{R}^3 \times \text{SO}(3)$  is digitized to allow a digitized motion. The configuration at a given moment of the object is the 6-plet  $\{i,j,k,l,m,n\}$  corresponding to the parameters  $(x,y,z,\varphi,\theta,\psi)$ . We allow movements only to neighboring cells and we compute the volume that the object sweeps during these infinitesimal movements. Thus the collision avoidance problem becomes a search problem for the allowed movements based on the volumes swept. This method is brute force but allows approximations of possible motions for an object. Further ways to reduce the computational load will be investigated.

*Keywords :* 3D solid representation, configuration space, path planning , collision avoidance.

*CSCC'99 Proceedings:* - Pages 5941-5948

## 1. Introduction.

Digital pictures have been the subject of research from the first days of computers evolved to the field of computer image analysis and recognition. Geometric properties of digital sets have been investigated and efforts have been focused on the topological properties of two-dimensional (2D) digital images. There exists a well-developed theory ([1][2]) for the topology of 2D digital sets.

With the evolution of computerized tomography and three-dimensional object scanning there was an increased need for three-dimensional (3D) object representation

tools. There was an analogous effort to study the topology and the geometric properties of 3D digital images [3][4]. The elements of 2D pictures are called pixels and cover a square unit of area. Equivalently the elements of 3D pictures are called voxels covering a cubic unit of volume.

Geometric properties of 3D pictures have been studied in an extensive bibliography. Specifically concepts like connectivity, adjacency, “thinning”, surfaces and components have been investigated [5][6][7][8]. The main target is to associate these properties with specific features of the object for recognition and identification.

Our task in this work is to use 3D representation of objects for motion planning and collision avoidance to be used in automated environments, teleoperations and robotics. In addition to this representation we use a 3D digitized version of the configuration space of a body to investigate the problems of planning and collision avoidance from this perspective.

## 2. 3D digital representation of solids.

For a 3D digital representation of a solid we create a 3-dimensional array of lattice points which correspond to the centers of equal unit cubes. In the case of motion planning the cubes are considered as units of matter comprising the object, occupying volume approximately equal to that of the object. The size of the unit cube is small enough to depict the details of the shape of the object. The lattice points in 3D pictures have integer dimensions and can be represented by a triad  $(i,j,k)$  corresponding to the center of each unit cube. We can define next the neighborhood of the point  $(i,j,k)$  using as base for the description the corresponding cube [3] :

1. Six "face neighbors"  $(i\pm 1,j,k)$ ,  $(i,j\pm 1,k)$  and  $(i,j,k\pm 1)$
2. Twelve "edge neighbors"  $(i\pm 1,j\pm 1,k)$ ,  $(i,j\pm 1,k\pm 1)$  and  $(i\pm 1,j,k\pm 1)$  the signs are chosen independently
3. Eight "corner neighbors"  $(i\pm 1,j\pm 1,k\pm 1)$  all three signs are chosen independently.

The topology is defined with respect to these neighboring cubes. The face neighbors are called "6-neighbors" and choosing this topology means that the point  $(i,j,k)$  is only connected to these 6-neighbors (we can go from  $(i,j,k)$  directly to each of these 6 points, but not to the other neighbors). In analogous way we can choose the topology of the "18-neighbors" with the neighbors of sets 1 and 2. Or the "26-neighbors" the points of all the three above sets.

In fact choosing a type of neighborhood for a digitized space has some implications when trying to interpret or replicate facts and results from continuous

topology [4]. Actually the 18-neighborhood leads to some paradoxes and is avoided. The "6-neighbors" and "26-neighbors" are better posed in terms of connectivity and curve description. This is mainly because they result respectively from two natural norms. The 6-neighborhood from the "grid distance" i.e. for two points  $(x,y,z)$  and  $(s,t,u)$  is defined as  $|x-s|+|y-t|+|z-u|$  (known for 2D as the city block metric). And the 26-neighborhood from the "lattice distance" defined as  $\max(|x-s|, |y-t|, |z-u|)$  (known for 2D as the chess board metric).

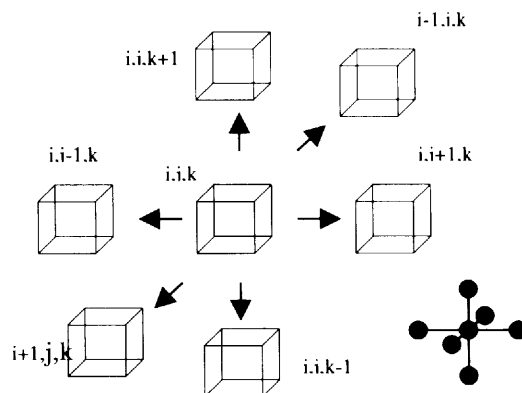


**Fig.1** The 6-neighbors and the corresponding lattice.

In Fig. 1 we can observe the "6-neighbors" and the corresponding lattice.

We assume that following one of the methodologies in literature we can construct a 3D representation of a solid. The initial data can result from a variety of sources e.g. a functional description of the surface  $f(x,y,z)=0$  of the solid. This will not be the usual case a more realistic assumption is to consider that we have a range of surface data obtained from a laser scanning device or a tomography. The range data are used then to create a triangulated mesh of the surface of the object. The 3D picture of the object is then created based on this surface model. One method could be, starting from an initial internal point to fill up the volume with unit cubes until the surface is reached. This is an analogy to the "inflated balloon method" [9] of range data triangulation (Fig. 2)

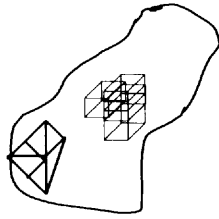


**Fig.2** Filling up a triangulated surface to create a 3D picture of an object

In fact for the purposes of motion planning and collision avoidance the triangulated surface should be crossed by the expanding cubic lattice except in cases where a face of a unit cube coincides with a triangle on

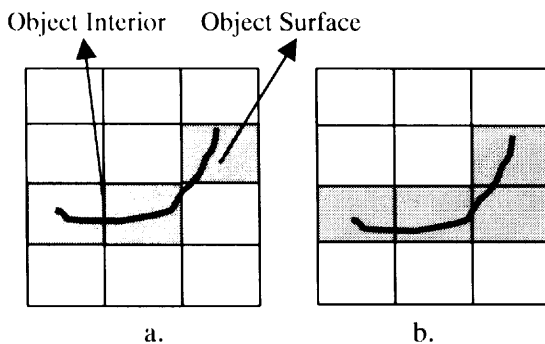


**Fig. 3** a) An accurate representation of an object b) a more appropriate representation for collision avoidance.

the surface. The accuracy of the model is not the first issue here instead taking the safe side is more important. There are cases where a digital 3D representation of the object is less accurate than other representations but more suitable for path planning and collision avoidance (Fig. 3).

Therefore the 3D representation of an object based on range data should contain the corresponding triangulated surface or in best cases coincide with a triangle element. The 3D lattice we obtain from a digitization as we described can be represented by a tree and the maximum number of the children nodes for each node depends on the type of topology we select (6-or 26-neighbor). The root node is considered to be the point that we start the object filling up process and the nodes that have the maximum possible number of children are internal to the object. Instead nodes without

maximum number of children nodes correspond to surface points of the object (Fig. 4).

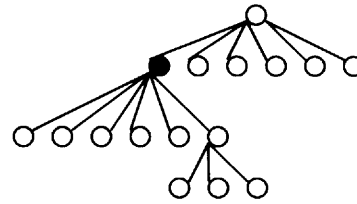


**Fig. 4** A tree structure representing an object with 6-neighbor topology. The black node is internal point.

### 3. Motion trajectories and configuration space of a solid object.

The state of a free solid object in  $\mathcal{R}^3$  at a certain moment can be represented by a point in  $\mathcal{R}^3$  corresponding to the position of the object reference frame and a point in  $SO(3)$  (the group of rotations) corresponding to the orientation of the object.

The configuration space of an object is the product  $\mathcal{R}^3 \times SO(3)$  and can be parameterized with the 6-plet  $(x, y, z, \varphi, \theta, \psi)$  where  $(\varphi, \theta, \psi)$  are the Euler angles [10][11].

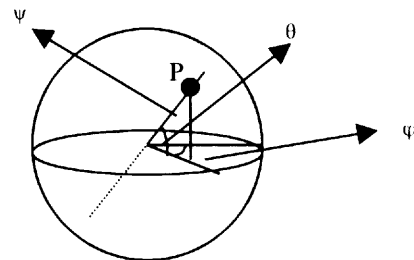


**Fig. 5** The  $SO(3)$  representation by the compact sphere.

There exists a geometric representation of  $SO(3)$  group by the compact solid sphere as in Fig .5.

The point P in Fig. 5 has coordinates  $(\varphi, \theta, \psi)$  measured from the origin and represents an orientation of a solid object at a certain moment. Angle  $\psi$  is measured as the distance from the origin of the compact sphere on the corresponding diameter. The points on the surface of the sphere are topologically identified with the diametrically opposite since  $-\pi < \psi \leq \pi$ . We have

also  $-\pi < 0 \leq \pi$  and  $-\pi < \varphi \leq \pi$ . A trajectory motion of a rigid body can be represented as a pair of trajectories in  $\mathcal{R}^3 \times \text{SO}(3)$  which could be parameterized by time  $(s(t), u(t))$  (Fig.6).

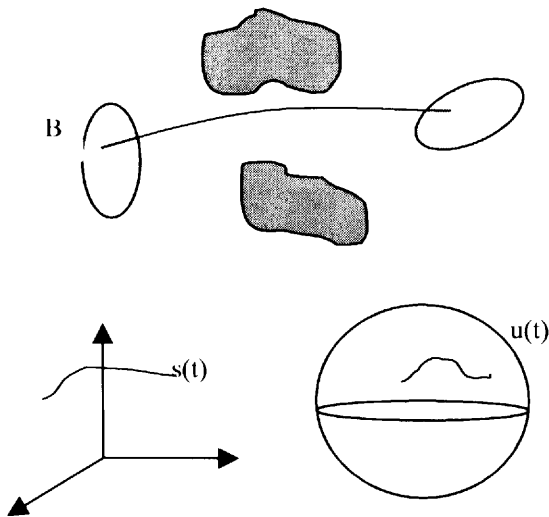


**Fig.6** The motion of a body and the corresponding position and orientation trajectories.

Next moving along the same framework of space representation we can digitize the configuration space of a rigid body and create an alternative mode for representing its motion.

Digitizing the product space  $\mathcal{R}^3 \times \text{SO}(3)$  is actually similar to what we have talked for the 3D representation of a solid object. In fact we can create a grid to digitize  $\mathcal{R}^3$  assuming that initially the unit cubes have the same edge length as the corresponding of grid for solid representation. This will facilitate the representation of translation motion. Grid with different size will result in more complicated problems which will be investigated in future work. A continuous trajectory in  $\mathcal{R}^3$  can be represented by a sequence of points  $P_0, P_1, \dots, P_n$  identified with the centers of unit cubes that the trajectory passes through (Fig. 7).

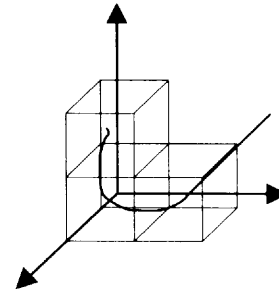


**Fig. 7** A continuous curve identified with the points  $P_0, P_1, P_2$ .

In an equivalent manner we can create a spherical lattice to digitize  $\text{SO}(3)$  see (Fig. 8).

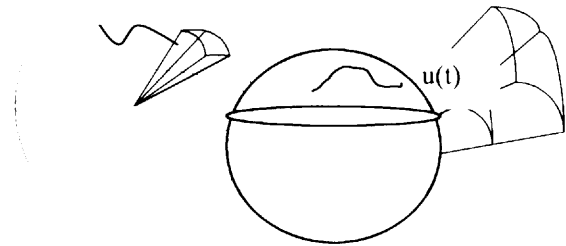


**Fig. 8** A trajectory in  $\text{SO}(3)$  group and the spherical grid

Important issue for the digitizing of the configuration space is the selection of the topology. A choice of 6-neighbor topology would mean that we move from a point  $P_h$  to a point  $P_{h+1}$  only if  $P_{h+1}$  belongs to the 6-neighbors of  $P_h$  (only one of the dimensions change). In fact the 6-neighbor topology is considered most appropriate for the digitization of  $\mathcal{R}^3$  and  $\text{SO}(3)$  because it simplifies the problems of path planning and collision avoidance to a certain degree. This is the case if we consider only one translational and one rotational parameter changing each time the body moves from one point in the configuration space to another. We can analyze the effects of the motion of the body much easier. Actually this way we decouple the motion of the body along and around the different axes.

#### 4. The changes of the 3D picture of a solid caused by the digitized motion.

Next we want to investigate the result of the digitized framework we developed. Actually for the purposes of path planning and collision avoidance we need to identify the volume that the 3D digital picture of the object sweeps during a transition from one pair point  $(P_h, O_h)$  in the configuration space to the next of a digitized trajectory  $(P_{h+1}, O_{h+1})$ .

We examine separately the case of translation and rotation. The case of translation is straight. In the 6-neighbor topology a transition from a point  $(i,j,k)$  to a point with only one coordinate change e.g.  $(i+1,j,k)$  will cause every unit cube in the set  $\Sigma$  that constitutes the 3D solid representation of the object to move in the  $x$  direction by one point in lattice. The result is that the volume  $V$  that the body sweeps during this elementary motion is the union of the original set  $\Sigma$  and the set of cubes  $\Sigma'$  resulting from the displacement of  $\Sigma$  by one cube (in this case in the direction of  $x$ )  $V = \Sigma \cup \Sigma'$ .

The situation for rotation is more complicated but with certain assumptions we can have more tractable results. Assume a translation from point  $O_h$  to a point next in the trajectory  $O_{h+1}$  (also in the 6-neighborhood of  $O_h$ ) in the digitized version of  $SO(3)$ . If the coordinates of  $O_h$  are  $(l,m,n)$  then we can assume a transition to the next point e.g.  $(l+1, m, n)$ .

If the spherical grid in  $SO(3)$  has a very small length  $\delta\alpha$  which corresponds to an infinitesimal angle. We can write down the transformation matrix for this infinitesimal rotation around the  $X$  axis [11]:

$$Rot(x, \delta\alpha) = \begin{bmatrix} 1 & 0 & 0 & 0 \\ 0 & 1 & -\delta\alpha & 0 \\ 0 & \delta\alpha & 1 & 0 \\ 0 & 0 & 0 & 1 \end{bmatrix}$$

This transformation changes also the position of the voxels of the initial 3D

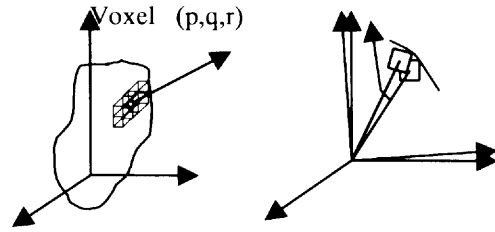


Fig.9 The effect of motion to the next point in  $SO(3)$  on a voxel of the object.

representation of the object. Assume a point in the lattice of the object with coordinates  $(p,q,r)$  we can visualize in Fig. 9 the effect of the infinitesimal rotation.

If the length of the lattice cube in  $\mathbb{R}^3$  is  $b$  then coordinates of the center of the voxel initially are in :

$$[p*b, q*b, r*b]$$

The coordinates of the center of the voxel after the infinitesimal rotation are

$$\begin{bmatrix} 1 & 0 & 0 & 0 \\ 0 & 1 & -\delta\alpha & 0 \\ 0 & \delta\alpha & 1 & 0 \\ 0 & 0 & 0 & 1 \end{bmatrix} \begin{bmatrix} p*b \\ q*b \\ r*b \\ 1 \end{bmatrix}$$

or

$$[p*b, q*b - \delta\alpha*r*b, r*b + \delta\alpha*q*b]$$

In Fig. 10 we can observe the change of the position and orientation of a voxel due to a transition from a point  $O_h$  to a neighbor point  $O_{h+1}$  (rotation around  $x$  axis) in the  $y$ - $z$  plane. If we restrict the motion of each voxel uniformly, during a transition from one orientation  $O_h$  to a neighboring one  $O_{h+1}$  then we can make conclusions about the volume that each voxel sweeps during such transition.

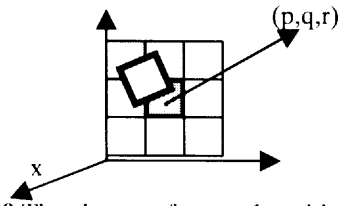


**Fig. 10** The change of a voxel position due to an infinitesimal rotation

Consider the minimal sphere that covers a voxel (unit cube). For a transition of the type  $(l, m, n)$  to  $(l+1, m, n)$  in the  $y$ - $z$  plane the voxel can have any orientation inside this sphere. There is no change in orientation in the other planes since the rotation is only around the  $x$  axis. If we want to restrict the motion of the voxel within the four neighboring voxels (Fig. 10 dark voxels) we can impose constraint on the size of the rotation. This can happen for the particular transition  $(l, m, n)$  to  $(l+1, m, n)$  which is positive and the voxel is located in the first quadrature ( $q \geq 1, r \geq 1$ ). For voxels in other quadratures we can constraint the motion of the voxel to the rest three sets of voxels each set corresponding to a quadrature.

When  $q \geq 1, r \geq 1$  (both coordinates positive) any positive rotation will move all the points of the cube within the quadrature defined by the two planes depicted with the solid line (Fig. 11). The minimal covering sphere for each voxel has a radius  $R = b\sqrt{2}/2$  ( $b$  the side of the unit cube). In order for the sphere to remain within the area of the three neighboring voxels (Fig. 11) the center of the sphere should remain within the dark area.

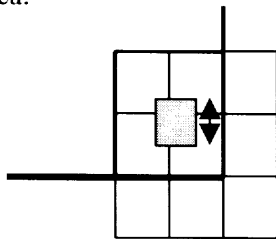


**Fig. 11** The constrained rotation.

We can impose an upper limit by requiring that the center of minimal containing sphere lies within the dark square with side  $(3 - \sqrt{2}) * b/2$ . This way the moving voxel

will at the most touch the sides of the neighbor voxels (solid lines). So we have the constraints :

$$\delta\alpha * r \leq (3 - \sqrt{2})/2$$

$$\delta\alpha * q \leq (3 - \sqrt{2})/2$$

Considering all three dimensions the following constraint guaranties that each voxel during an elementary rotational motion will sweep at most four neighboring voxels :

$$|\delta\alpha| = (3 - \sqrt{2})/2 * \min(1/|p|, 1/|q|, 1/|r|)$$

Therefore with a lattice  $\delta\alpha$  for  $SO(3)$  that satisfies the above constraint we can always have that the motion of a voxel during an infinitesimal rotation around one axis will at the most sweep four neighboring voxels depending on the quadrature of the voxel.

We have defined therefore the volume that a 3D picture of an object sweeps during a

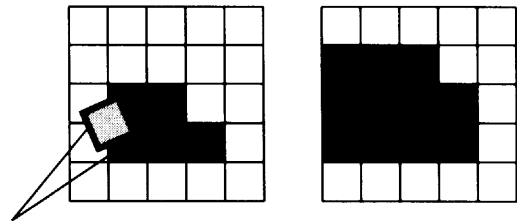


**Fig. 12** Example of a rot-solid in two dimensions left is the original solid

motion from one point  $O_h$  to a neighboring one  $O_{h+1}$  in  $SO(3)$ . In Fig. 12 we can see the volume that the 3D representation sweeps for a one point transition in the digitized  $SO(3)$  around axis  $x$ . We call the resulting volume *rot-solid* for the transition  $(l, m, n) \rightarrow (l+1, m, n)$ . The *rot-solid* is an extension of the original 3D representation that describes a particular rotational transition in the  $SO(3)$  grid. It is actually a volume envelope that includes the 3D solid during this elementary motion.

## 5. The 3D picture and a motion trajectory.

A motion trajectory of a rigid body within the work frame we have described can be

represented as a sequence of pairs of points  $(P_0, O_0), (P_1, O_1), \dots, (P_m, O_m)$  such that  $P_0, P_1, \dots, P_m \in \mathcal{R}^3$  and  $O_0, O_1, \dots, O_m \in SO(3)$ . We can also assume that the pair  $(P_h, O_h)$   $h \in \{1, \dots, m\}$  corresponds to a time  $t_h$ . This means that the trajectory can be given a time parameterization allowing this way the motion planning and the connection of these type of representation with dynamic modelling.

There is a main implicit constraint that is imposed on this type of trajectory representation with voxels. Consequent points that belong to a sequence representing a trajectory are unit-neighbors. This means that  $P_h$  belongs to the neighborhood of  $P_{h-1}$  and  $O_h$  in the neighborhood of  $O_{h-1}$ . Where neighbor means 6- or 26- neighbor. We indicated in the previous section that the 6-neighbor topology is more appropriate to describe the result of a elementary motion. We will leave the investigation of other topologies for future works.

Assume a motion step from  $(P_h, O_h)$  to  $(P_{h+1}, O_{h+1})$  such that if  $P_h = (i, j, k)$  then  $P_{h+1}$  can only be one of the following points in  $Z^3$  ie  $P_{h+1} = (i \pm 1, j, k)$  or  $(i, j \pm 1, k)$  or  $(i, j, k \pm 1)$ . Equivalently if  $O_h = (l, m, n)$  then  $O_{h+1} = (l \pm 1, m, n)$  or  $(l, m \pm 1, n)$  or  $(l, m, n \pm 1)$ . In this case the motion can be decoupled we can consider first the translational motion  $(P_h \rightarrow P_{h+1})$  and then the rotational  $(O_h \rightarrow O_{h+1})$  or vice-versa. This is maybe a good way to study the details of the motion of the body but does not represent reality. The natural way is to have both translational and rotational motion executed contemporarily since each point is associated with a time instance  $t_h$  that marks the instantaneous position and orientation of the body.

The motion from  $P_h$  to  $P_{h+1}$  causes the rigid body to sweep a part of  $\mathcal{R}^3$ . The total volume which is swept is the union of the set of voxels occupied by the body at position  $P_h$  and the set of voxels occupied at position  $P_{h+1}$ . The motion for example from  $(i, j, k)$  to  $(i+1, j, k)$  is a translation of all the voxels by one voxel to the direction of  $x$  coordinate. Since the translation is linear the

volume swept during this motion is the union of the voxels at  $P_h$  and at  $P_{h+1}$ .

The volume swept by the infinitesimal rotation is the corresponding rot-solid for the particular rotational movement from  $O_h$  to  $O_{h+1}$ . Contemporary translation and rotation means to superimpose the two motions. To compute the corresponding swept volume by the two motions we can translate the rot-solid by one voxel to the direction of  $P_h$  to  $P_{h+1}$ . The union of the set of voxels which corresponds to the rot-solid at position  $P_h$  and the set of voxels which corresponds to the rot-solid at position  $P_{h+1}$  is the maximum possible swept volume by the combined motion. This gives an envelop for the volume swept by a combined translational and rotational move since the full rotation is not completed before reaching  $P_{h+1}$ . Consider the example of Fig.12 where we indicate the rot-solid for an infinitesimal rotation from  $O_u = (i)$  to  $O_u = (i+1)$ . The rotations allowed in 2-dimensional space are only 1-dimensional (around the axis vertical to the plane of the text). Then if we superimpose the described infinitesimal rotation with a translation from point  $P_u = (i, j)$  to  $P_{u+1} = (i+1, j)$ , the result of the swept area is given by the union of the rot-solid at  $P_u$  and  $P_{u+1}$  (Fig. 13). Thus for motion planning or collision avoidance of the body in Fig. 13 from the pair point  $(P_u, O_u)$  to  $(P_{u+1}, O_{u+1})$  we have to consider the swept area indicated in Fig. 13.

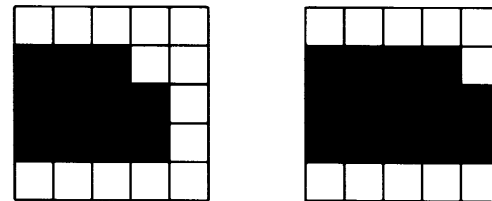


**Fig. 13** The result of combining translational and rotational motion

## 6. Conclusions

In this work we have created a framework to use 3D picture of objects to investigate path planning and collision avoidance problems. We constructed a digitized version of the configuration space  $\mathcal{R}^3 \times$

SO(3) and this way we were able to decompose any continuous trajectory to a sequence of pairs of points.

One point which may not be so obvious is that for every point  $O_h$  in the digitized SO(3) we have to consider a different 3-D representation of the solid. Thus if SO(3) is digitized with  $n$ -points then we should have  $n$  representations of the body each one for a different orientation. On the top of this we should have  $6n$  rot-solids corresponding to all the possible rotational transitions from each orientation to the 6 neighboring. This is necessary if we want to have a refined representation of the rotational movements. If we want to avoid this we have to compromise with a general rot-solid represented by the minimal covering sphere for the whole body. This has already been investigated in collision avoidance problems.

In our proposed methodology we can compute in advance the 3D representations of an object for each point in SO(3) and all the related transitions ( $7 \cdot n$  3D solids). This have to be done for all the objects whose geometry is known and are present within a restricted area of interest.

Thus the path planning and collision avoidance problems end up as pure search problems.

We can further investigate ways to reduce this brute force searching load by exploiting different facts. For example we can investigate the relative sizes of the objects as well as start the search from points in the surface of 3D representation



**Fig. 14** Three possible cases of two object relative positions  
since there are only three possible cases of relative positions between two objects (Fig. 14).

1. No collision.
2. Collision with surfaces intersection

3. The smaller body is within the bigger body.

When there is an obvious difference in size we can just investigate the surface points of the smaller object first against all the points on the surface of the second body and then against all the points in the interior. Further computational complexity analysis is required to assess the capabilities of this framework.

### References.

- [1] Rosenfeld, A. 1979 Digital Geometry, in "Picture Languages" Chap.2 Academic Press, New York.
- [2] Tzourlakis, G. and Mylopoulos, J. 1973 Some results on computational topology, ACM Journal 20. 439-455
- [3] Rosenfeld, A. 1981 "Three-Dimensional Digital Topology", Information and Control 50, 119-127.
- [4] Kong, T.Y. and Rosenfeld, A. 1989 "Digital Topology : Introduction and Survey" Computer Vision Graphics and Image Processing 48. , 357-393.
- [5] Morgenthaler, D. G. and Rosenfeld, A. 1981 Surfaces in three-dimensional digital-images, Information and Control 51, 227-247.
- [6] Mylopoulos, J. P. and Pavlidis, T. 1971 On the topological properties of quantized spaces I : The notion of dimension. ACM Journal 18 239-246
- [7] Mylopoulos, J. P. and Pavlidis, T. 1971 On the topological properties of quantized spaces II : Connectivity and order of connectivity. ACM Journal 18 247-254
- [8] Tsao, Y. F. and Fu, K.S. 1981 A parallel thinning algorithm for 3D pictures, Computer Graphics and Image Processing 17, 315-331.
- [9] Chen, Y. and Medioni, G. 1995 Description of Complex Objects from Multiple Range Images Using an Inflating Balloon Model, Computer

Vision and Image Understanding, Vol  
61 No3 325-334.

- [10] Greenwood, D. T. 1965 Principles  
of Dynamics. Prentice Hall
- [11] Graig , J. J. 1986. Introduction to  
Robotics Mechanics and Control.